

MECHANISMS OF PHOTODYNAMIC KILLING OF CANCER CELLS BY PHOTODITHAZINE

R. Alzeibak, N.N. Peskova, O.M. Kutova, S. Shanwar, I.V. Balalaeva*

Institute of Biology and Biomedicine, Lobachevsky State University of Nizhny Novgorod, Nizhny Novgorod, 603950, Russia.

* Corresponding author: irin-b@mail.ru

Abstract. Photodynamic therapy (PDT) is a promising approach in the treatment of various tumors. The presence of three essential components: a photosensitizer, a light source and oxygen is required for generating reactive oxygen species and subsequent tumor destruction. In this study, we investigated the cell death pathway induced by Photodithazine (PD) mediated photodynamic therapy (PD-PDT). We found that PD localizes in the endoplasmic reticulum and Golgi apparatus of cancer cells. Upon irradiation at 20 J/cm², PD induced death of tumor cells at concentrations exceeding 100 nM. Based on dying cell morphology, exposure of phosphatidylserine to the cell surface, presence of phosphorylated form of mixed lineage kinase domain like pseudokinase (pMLKL) and protective action of pan-caspase inhibitor and inhibitor of receptor-interacting protein kinase 1 (RIPK1), we hypothesize that Photodithazine forces cells to enter mixed-type cell death with features of apoptosis and necroptosis.

Keywords: Photodynamic therapy, photodithazine, cell death, necroptosis.

List of Abbreviations

μm – Micrometer
μM – Micromolar
AnxV – Annexin V
DFO – Deferoxamine
DMEM – Dulbecco's Modified Eagle's medium
ER – Endoplasmic reticulum
fer-1 – Ferrostatin-1
IC₅₀ – The concentration of PD resulting in 50% inhibition of cell culture growth
MLKL – Mixed lineage kinase domain-like protein
nec-1 s – Necrostatin-1 s
nm – Nanometer
PD – Photodithazine
PDT – Photodynamic therapy
PI – Propidium Iodide
pMLKL – Phosphorylated MLKL
PS – Photosensitizer
ROS – Reactive oxygen species
UPR – Unfolded Protein Response
zVAD-fmk – Carbobenzoxy-valyl-alanyl-aspartyl-[O-methyl]-fluoromethylketone

Introduction

Photodynamic therapy (PDT) is an emerging approach for cancer therapy, that takes advantage of the optical features of a non-toxic

photosensitive dye, otherwise known as a photosensitizer (PS). PS is capable of generating reactive oxygen species (ROS) in the presence of tissue oxygen upon local exposure to light with a wavelength corresponding to its absorption maximum (Dolmans et al., 2003). The resulting ROS, depending on where they are generated, can directly cause damage to organelles and membranes of local cells (Bacellar et al., 2015). Therefore, the type of PS and its intracellular distribution are critical factors in PDT's successful applications (Hamblin, 2020).

After light absorption by PS in its ground state, it becomes activated to a short-lived (nanoseconds) first excited singlet state, then it can lose the absorbed energy by emitting light (fluorescence) or as heat by internal conversion. The excited singlet state PS can also form the relatively long-lived (microseconds) excited triplet-state PS via intersystem crossing. Subsequently, the excited triplet state PS can undergo two kinds of reactions with surrounding molecules (Robertson et al., 2009). In type I photochemical reaction, the excited triplet state PS can react directly with a substrate, like cell membrane, and transfer an electron or a proton to form radicals. Further, these radicals may react with cellular oxygen and produce reactive oxygen species (ROS), such as peroxides, su-

peroxide ions ($O_2^{\bullet-}$), and hydroxyl radicals (OH^{\bullet}) and initiating free radical chain reactions (Abrahamse & Hamblin, 2016). On the other hand, in type II photochemical reaction, the excited triplet state PS can transfer its energy directly to molecular oxygen, which by itself is a triplet in its ground state (3O_2), producing an excited-state singlet oxygen (1O_2), the most imperative reactive species in PDT-mediated cytotoxicity, which reacts with several biological molecules, including lipids, proteins, and nucleic acids (Greer, 2006).

The cellular response to photodamage varies strongly according to several defining factors with PS localization within the cell playing the major role. Intracellular localization of PS defines PS site of action, differs depending on PS type, and plays a vital role in determining the fate of the cell (Van Straten et al., 2017). PS characteristics are generally responsible for its localization toward cellular organelles such as the plasma membrane, lysosomes, mitochondria, Golgi apparatus or endoplasmic reticulum (ER) (Castano et al., 2004).

The PDT-induced production of ROS and 1O_2 leads to tumor destruction by multifactorial mechanisms. The first mechanism is the direct killing of tumor cells by PDT, alongside affecting tumor vasculature and causing vessel shutdown, and consequently depriving tumor cells of oxygen and nutrients (Wang et al., 2012). The second, most important, mechanism is the rapid recruitment and activation of immune cells leading to tumor elimination, which is currently under extensive research (Donohoe et al., 2019).

Recently, it has been established that PDT results in triggering different mechanisms of cell death, that can be either non-regulated cell death (accidental) or regulated, including necrosis, apoptosis (Shams et al., 2015), necroptosis (Dos Santos, et al., 2020), ferroptosis (Turubanova et al., 2019), and autophagy-dependent cell death (Garg et al., 2013), allowing PDT to treat various mechanisms of resistance, exhibited by malignant cells (Dos Santos et al., 2019). A single PS may trigger multiple types of cell death under different treatment conditions. Typically, high photodamage (high PS

concentration and/or high dose light) induces necrosis. Thus, moderate photodamage is expected to induce regulated cell death modalities, that are capable of eliciting immune responses with systemic impact, making PDT a more appealing and relevant therapeutic alternative (Donohoe et al., 2019).

The aim of the present study was to define the type and characterize the mechanism of cell death induced by PDT treatment with a clinically approved photosensitizer – Photodithazine® (PD). We investigated the involvement of apoptosis and necroptosis in cell death triggered by PD -PDT using inhibitory analysis, analysis of phosphatidylserine externalization and detection of phosphorylated form of mixed lineage kinase domain like pseudokinase (pMLKL).

Materials and methods

Cell lines. Experiments were performed on two human tumor cells lines: human skin epidermoid carcinoma A431 and human transitional cell carcinoma of the urinary bladder T24 (Russian Collection of Cell Cultures). Cells were cultured in Dulbecco's modified Eagle's medium (DMEM, PanEco, Russia) supplemented with 2 mM glutamine and 10% (v/v) fetal bovine serum (PanEco, Russia) in 5% CO₂ atmosphere at 37 °C.

Photosensitizers. Photodithazine® (PD), which is the bis-N-methylglucamine salt of chlorin e6 (Veta-grand, Russia), was used as a photosensitizer for photodynamic treatment.

Analysis of intracellular distribution of Photodithazine. The intracellular distribution of Photodithazine was visualized using an Axio Observer Z1 LSM-710 DUO NLO laser scanning microscope (Carl Zeiss, Germany). For the study, A431 cells were seeded in glass-bottom 96-well plates at a density of 4×10^3 cells/well and grown overnight at 37°C in 5% CO₂ atmosphere. Later on, the cells were incubated with PD at concentration of 10 μM in serum-free cell culture medium for 4 h. After that, PD containing medium was replaced with fresh complete cell growth medium. Colocalization analysis

was conducted to identify PD's localization in individual cellular organelles. Chemical dyes LysoTracker green (0.5 μ M), BODIPY FL C5-ceramide with BSA (5 μ M), ER-Tracker Green (BODIPY FL glibenclamide) (0.5 μ M) (Life Technologies, USA), and genetically transformed cell line A431 expressing the fluorescent protein HyPer in the cytoplasm or mitochondria were used for visualizing the lysosomes, Golgi apparatus, endoplasmic reticulum (ER), cytoplasm and mitochondria, respectively. Dyes were added to living cells, pre-incubated with PD. The staining procedure was performed according to manufacturer's instructions. The cells were excited at 488 nm and 633 nm to visualize stained organelles and PD, respectively. Subsequently, fluorescence emission was registered in the range of 500–560 nm for stained organelles and 650–735 nm for PD.

Analysis of dark toxicity and photodynamic activity. To study dark cytotoxicity and photodynamic activity of Photodithazine, A431 and T24 cells were seeded in 96-well plates at a density of 6×10^3 cells/well and grown at 37°C in 5% CO₂ atmosphere overnight. Afterwards, the media in all the wells was replaced with serum-free media containing PD at the concentration range of 0.001–50 μ M and incubated for 4 hours (serum-free media without PD was added to control wells), followed by either keeping under dark conditions (for the dark cytotoxicity study) or irradiation with a light dose of 20 J/cm² in photosensitizer-free medium using a LED light source (at wavelength 655–675 nm) at a power density of 32 mW/cm² to induce photodynamic activity (Shilyagina et al., 2014). Finally, the cells were cultured in complete medium for 24 hours and cell viability was analyzed by MTT assay (Alfa Aesar, UK) according to the manufacturer's instructions. MTT reagent was added to the growth medium at a concentration of 0.5 mg/ml and the cells were incubated for 4 h. Then, to dissolve the formed formazan crystals, the culture medium was replaced with 200 μ l of dimethyl sulfoxide (DMSO). The optical density of each well was measured using Synergy MX Plate Reader (Bi-

oTek, USA) at 570 nm. Data analysis and calculation of the IC₅₀ values (the concentration of PD resulting in 50% inhibition of cell culture growth at the selected irradiation dose) were acquired using the GraphPad Prism software (v. 6.01, GraphPad Software, Inc, USA).

Assessment of cellular morphology and rate of cell membrane permeabilization. A series of experiments was carried out to monitor membrane permeabilization and cellular morphological changes after short-term and intense photodynamic exposure, in order to analyze how fast cell death can be induced after PDT application.

For this purpose, A431 and T24 cancer cells were seeded in a glass-bottom Petri dish, then PD was added to the cells at a pre-determined concentration to result in more than 90% inhibition of cell culture growth (IC > 90) – 10–6 M, followed by irradiation through the objective of confocal microscope Axio Observer Z1 LSM-710 DUO NLO (Carl Zeiss, Germany) with a light dose of 20 J/cm² (655–675 nm). Immediately after irradiation, propidium iodide (PI) was added to the incubation medium, which penetrates only into cells with disrupted plasma membrane integrity, making it possible to monitor the dynamics of membrane permeabilization in irradiated cells.

Identifying of cell death type by inhibitory analysis. To determine the mechanism of cell death induced in cancer cells by PD-PDT, the method of inhibitory analysis was used with the following compounds: pan-caspase inhibitor carbobenzoxy-valyl-alanylasparyl-[O-methyl]-fluoromethylketone (zVAD-fmk), which inhibits apoptosis; inhibitor of receptor-interacting protein kinase 1 (RIPK1) necrostatin-1s (Nec-1s), which inhibits necroptosis; inhibitor of ROS and lipid peroxidation ferrostatin-1 (Fer-1) and iron chelator, deferoxamine (DFO), which inhibit ferroptosis (Sigma-Aldrich, USA).

Cells were seeded in 96-well plates at a density of 6×10^3 cells/well and grown at 37 °C in 5% CO₂ atmosphere overnight. Then, the cell culture medium was replaced with 100 μ l of a

serum-free medium containing PD in a concentration corresponding to IC₅₀ and inhibitors of apoptosis (25 μ M zVAD-fmk), ferroptosis (1 μ M Fer-1 or 10 μ M DFO) or necroptosis (20 μ M Nec-1s) and incubated for 4 hours, after that the medium was again replaced with complete cell culture medium without PD, but with the respective cell death inhibitor. Afterwards, the cells were irradiated at a dose of 20 J/cm² or kept outside the CO₂ incubator in the dark for an equal time, then they were incubated for 13 hours and cell viability was analyzed by MTT assay. Variants of treatment were compared by t-criteria with Bonferroni correction using the GraphPad Prism 6 software.

Flow cytometry analysis of phosphatidylserine externalization. To analyze phosphatidylserine externalization, A431 cells were seeded in 6-well plates at a density of 4×10⁵ cells/well and grown at 37 °C in 5% CO₂ atmosphere overnight. Next, the cell culture medium in the wells was replaced with serum-free medium with the PD at a concentration corresponding to IC₅₀ and incubated for 4 hours (media without PD was added to the control wells), followed by either keeping in the dark or irradiation with a light dose of 20 J/cm² in photosensitizer-free medium (at wavelength 655–675 nm). Later on, the cells were cultured in complete medium for 13 hours. Then, cells were harvested and stained with AnxV-FITC and PI using a FITC Annexin V Apoptosis Detection Kit I (Invitrogen, USA), according to the manufacturer's instructions. The samples were analyzed using a cell sorter FACS Aria III (BD, USA).

pMLKL protein detection by Western blot. A431 cells were seeded in 6-well plates at a density of 4×10⁵ cells/well and grown at 37 °C in 5% CO₂ atmosphere overnight. Next, the cell culture medium in the wells was replaced with serum-free medium with PD at a concentration corresponding to IC₅₀ and incubated for 4 hours (media without PD was added to control wells), followed by either keeping in the dark or irradiation with a light dose of 20 J/cm² in photosensitizer-free medium (at wavelength 655–675 nm). Later, the cells were cultured in

complete medium for 13 hours. After that, the cells were lysed in ice-cold lysis buffer (0.5% NP-40, 0.5% Triton X-100, 50 mM Tris-HCl pH 7.5, 150 mM NaCl, 2 mM EDTA and cOmplete™, Mini Protease Inhibitor Cocktail, 1 tablet per 10 ml buffer), then were incubated on ice for 30 minutes. For electrophoresis, samples of cell lysates were diluted at a ratio of 4:1 with five-fold sample buffer containing 250 mM Tris-HCl pH 6.8, 10% sodium dodecyl sulfate (SDS), 0.5% bromophenol blue, 50% glycerol and 20% β -mercaptoethanol, and heated for 20 minutes at 99°C. 8% polyacrylamide gels were used for protein separation, using Running buffer (192 mM Tris and 25 mM glycine pH 8.3 and 0.1% SDS). Later on, protein bands were transferred from the gel onto Immobilon®-P PVDF membranes (Merck, Germany), which subsequently were blocked for 3 hours in TBS Buffer (20 mM Tris and 150 mM NaCl) pH 7.5, containing 5% skim milk powder, then probed with the following primary antibodies: anti-MLKL rabbit polyclonal antibodies c-terminal (1:1000, Abcam, UK) for the detection of mixed lineage kinase domain-like protein (MLKL); anti-MLKL (phospho S345) rabbit monoclonal antibodies (pMLKL) (1:1000, Abcam, UK) for the detection of phosphorylated MLKL and anti-beta tubulin rabbit polyclonal antibodies (1:1000, Abcam, UK) for normalizing blots. After washing, the membranes were incubated with secondary antibody (anti-rabbit IgG from donkey, 1:4000, GE Healthcare, UK); for visualization protein bands, chemiluminescent substrate Clarity Max™ Western ECL (Bio-Rad, USA) was used and luminescence was registered using a ChemiDoc™ Imaging System (Bio-Rad, USA).

Results

Subcellular distribution of Photodithazine. Photodithazine is characterized by fast penetration into tumor cells, consequently, incubation for 4 hours led to high level of PD accumulation in cells. Analysis of the photosensitizers' intracellular localization showed that the main site of PD accumulation in A431 cells are cellular membrane structures, such as the ER and the

Golgi apparatus (Fig. 1). Whereas, co-localization of PD with cellular organelles such as mitochondria or lysosomes was not found. This distribution in cells is consistent with the physicochemical characteristics of PD, which is an amphiphilic compound with pronounced lipophilic properties.

Photodynamic activity of Photodithazine. The study of dark toxicity showed no effect of PD on cell viability in T24 cells culture at concentrations up to 50 μM . In the case of A431 cells, a higher toxic effect was observed: incubation with PD at concentrations exceeding 5 μM led to a decrease in the viability of cells (Fig. 2).

Analysis of cell viability of both cell lines showed similar dose-dependent responses to the photodynamic treatment with PD (Fig. 2). Irradiation with a wavelength of 655-675 nm at a dose of 20 J/cm² led to cell death at PD concentrations above 100 nM. IC₅₀ values calculated based on dose-effect curves for PD-PDT are summarized in Table 1.

Changes in cellular morphology and cell membrane permeabilization under PD-PDT treatment. The high intensity PD-PDT treatment of cells led to the appearance of pronounced morphological changes even over a very short time. Morphological change analysis in A431 and T24 cells upon PD exposure showed granulation of the cytoplasm, cell swelling and “fixation” (Fig. 3).

In order to analyze in detail the rate of tumor cells death upon PD exposure, a series of experiments was carried out to monitor the membrane permeabilization of cells after a short-term intense photodynamic effect. The response of cells to the photodynamic treatment is manifested in a breach of the membrane integrity shortly after irradiation. In 10 minutes after irradiation, the staining of cell nuclei with PI was quite pronounced, and after 20 minutes it reached a maximum (Fig. 3).

Type of the cell death by inhibitory analysis. In order to determine the type of cell death induced by PD-PDT, an inhibitory analysis was

performed using compounds that selectively inhibit induction of apoptosis, necroptosis, and ferroptosis. In the case of A431 cells, the pan-caspase inhibitor zVAD-fmk and necrostatin-1s, which prevent induction of necroptosis, increased the viability of the A431 cell culture upon PD exposure (Fig. 4). In the case of T24 cells, necrostatin-1s significantly increased the viability of the T24 cell culture. Additionally, a tendency towards higher cell viability under the effect of zVAD-fmk was revealed for T24 cell line (Fig. 4). It is noteworthy that the cytoprotective effect of ferroptosis inhibitors (lipid-radical trapping antioxidant (ferrostatin-1) or an iron chelator (DFO)) was absent upon PD exposure.

Externalization of phosphatidylserine on the outer leaflet of membranes of photosensitized cells. Phosphatidylserine exposure on to the external leaflet of the plasma membrane is widely observed during apoptosis, however, recently the possibility of exposure of phosphatidylserine has been shown in non-apoptotic forms of regulated cell death, such as necroptosis (Zargarian et al., 2017). To determine the externalization of phosphatidylserine in response to the photodynamic effect of PD, cells were stained with phosphatidylserine-binding protein annexin V conjugated with fluorescent dyes FITC and PI, which penetrates only dead cells with breached plasma membrane integrity. 13 hours after irradiation of A431 cells treated with PD, a large amount, up to 40–50%, of living cells (PI-negative) stained with AnxV and presumably at the stage of early apoptosis was observed (Fig. 5). This confirms the results of the inhibitory analysis. The quantity of dead cells stained with both dyes (PI-positive AnxV-positive) reached 25-30%, but this method does not allow separating cells that have died through apoptosis, necroptosis, or other types of cell death.

Phosphorylation of a mixed lineage kinase domain-like protein (MLKL) triggered by PD-PDT. The most important participants in the signaling cascade in necroptosis are receptor-interacting protein kinases 1 and 3 (RIPK1, 3), which are involved in the phosphorylation of

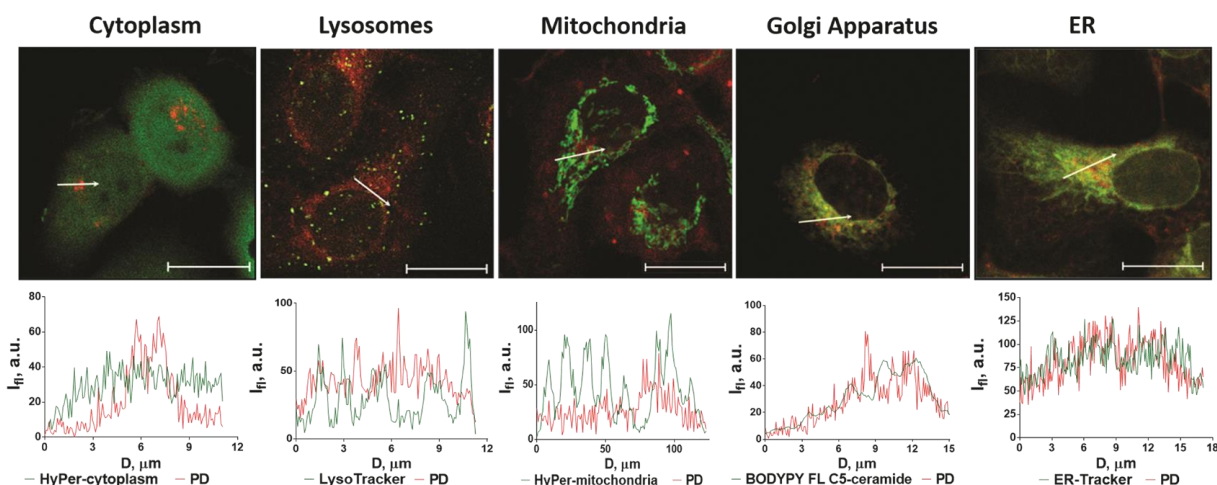


Fig. 1. Analysis of intracellular localization of Photodithazine (PD) in A431 cells. The cells were incubated with PD (10 μM) for 4 hours and then stained with the following dyes: LysoTracker Green for lysosomes; ER-Tracker for ER and BODYPY FL C5-ceramide complexed to BSA for Golgi apparatus. For cytoplasm and mitochondria visualization, the genetically transformed A431 cells expressing fluorescent protein HyPer in cytoplasm or mitochondria were used. Top row: confocal images for merged fluorescent channels (red fluorescence of PD, green fluorescence of the labeled organelle or compartment) are presented. Scale bars, 20 μm . Bottom row: fluorescence signal profiles along the lines indicated by the white arrow on the images are shown. I_f : fluorescence intensity; D: distance along the specified lines

the MLKL protein. Oligomers of phosphorylated MLKL are translocated into the plasma membrane, increasing its permeability and subsequent rupture (Dhuriya & Sharma, 2018). For specific confirmation of the involvement of necroptosis in cell death induced by PD-PDT, we used Western blot method. We have shown that irradiation of A431 cells treated with PD resulted in an increase in the amount of phosphorylated form of MLKL (pMLKL) and, therefore, the induction of necroptosis (Fig. 6), which is also consistent with the result of inhibitory analysis.

Discussion

Analysis of the cell death mechanisms induced in cancer cells by photodynamic therapy is of great practical value for increasing the efficiency of PDT, reducing side effects, and searching for approaches to regulating the types of tumor cells death, especially in cases of cancer resistant to treatment.

The cellular response to photodamage depends on several factors, the key of which is the subcellular distribution of PS (Oliveira et al.,

2011). Depending on the characteristics of PS, it predominantly localizes in plasma membrane, lysosomes, mitochondria, the Golgi apparatus, or ER. Cytoskeleton and cell adhesion components have also been described as targets for PS (Juarranz et al., 2008). Depending on the charge, cationic compounds accumulate in mitochondria, while anionic molecules are found in lysosomes. Lipophilicity also affects subcellular localization; amphiphilic and lipophilic compounds predominantly accumulate in the perinuclear region and penetrate into the membrane structures, such as, ER and mitochondria (Van Straten et al., 2017). This leads to the fact that the primary targets of photodynamic effects depend on physicochemical properties of PS. Therefore, the molecular pathways triggered by irradiation can vary and lead to different consequences.

Photodithazine is an amphiphilic compound (Brilkina et al., 2018), and the relative lipophilic properties of PD determine its localization in different intracellular membrane compartments, such as the ER and Golgi apparatus (Fig. 1). Similar distribution of PD has been

The half-inhibitory concentration of Photodithazine for A431 and T24 cell culture upon irradiation with a light dose of 20 J/cm²

Cell line	Half-maximum inhibitory concentration of Photodithazine IC ₅₀ *, μM
A431	0,099 (0,076; 0,13)
T24	0,085 (0,061; 0,093)
* – to calculate IC ₅₀ , a lognormal distribution model was used, the mean values and 95% confidence interval are indicated	

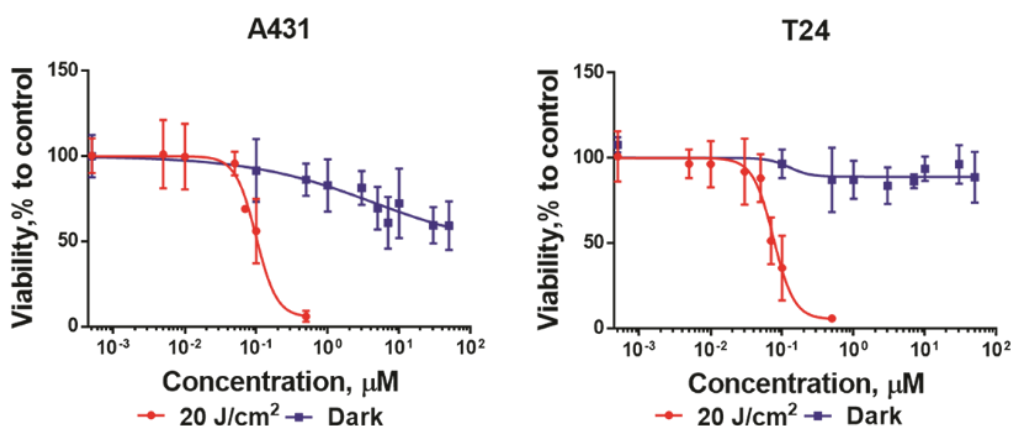


Fig. 2. Dark toxicity and photodynamic activity of Photodithazine (PD) against A431 and T24 cell lines as a function of PD concentration. The cells were incubated with PD for 4 h and then were irradiated at a dose of 20 J/cm² (655–675 nm, 32 mW/cm²). For dark cytotoxicity assessment, the plate was kept without irradiation. Cell viability was analyzed 24 h after irradiation by MTT assay

previously reported for a number of other cancer cell lines, including mouse glioma GL261 (Turubanova et al., 2019) and human cervical adenocarcinoma HeLa-Kyoto (Brilkina et al., 2018). Irradiation of PD pre-treated cells resulted in rapid cell death with IC₅₀ less than 0.1 μM (Fig. 2, table 1).

Nowadays, it is recognized that PDT can induce various types of accidental and regulated cell death. However, the factors, which determine the type and mechanism of cell death are not yet clear and might include the PS type, subcellular localization of PS, the dose of light and fluence rate applied, and also the intrinsic characteristics of tumor type (Van Straten et al., 2017).

We have shown that PD-PDT causes fast breach in A431 and T24 cell membrane integrity (Fig. 3).

To establish that cell death was not an outcome of an unregulated rupture of the cell mem-

brane (necrosis) due to an intense photodynamic exposure, we applied several complementary approaches.

Our results demonstrated that PD-PDT can trigger two different type of regulated cell death – apoptosis and necroptosis confirmed with following approaches: the inhibitors of apoptosis (pan-caspase inhibitor zVAD-fmk) and necroptosis (RIPK1 inhibitor necrostatin-1s) increased cell viability upon PD exposure; phosphatidylserine exposure on the external leaflet of the plasma membrane after PD-PDT was shown, which refer to induction of both apoptosis (Segawa & Nagata, 2015) and necroptosis (Zargarian et al., 2017; Shlomovitz et al., 2019); and phosphorylation of MLKL (pMLKL) was triggered by PD-PDT, as a hallmark of necroptosis induction (Samson et al., 2020).

Depending on our own and literature data, we have proposed that the physicochemical

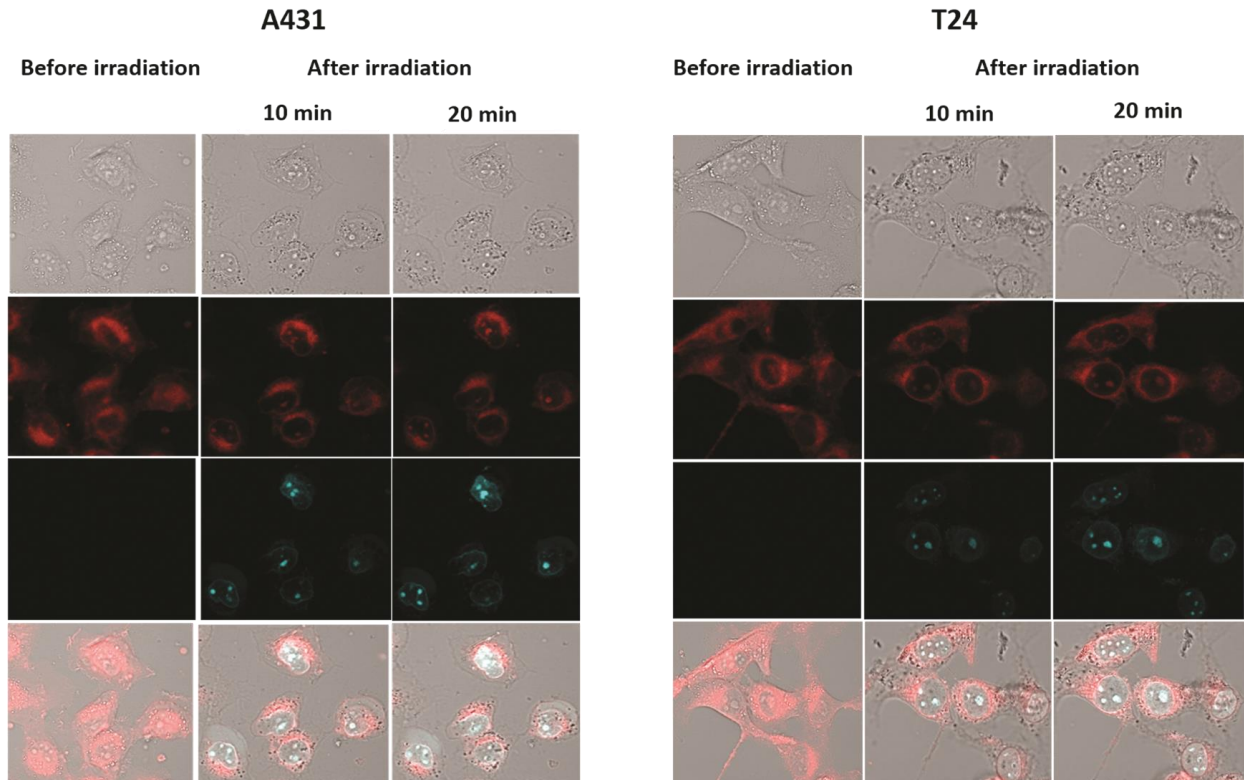


Fig. 3. Assessment of cell-membrane permeabilization rate of A431 and T24 cells pre-treated with PD at a concentration of 10^{-6} M and irradiated at a dose of 20 J/cm^2 . The incubation medium contains PI, which penetrates into cells with disrupted plasma membrane integrity. Confocal images in transmitted light, fluorescence of PD (red), fluorescence of PI (blue), and merged fluorescent channels are presented. Images size $50 \times 50 \mu\text{m}$

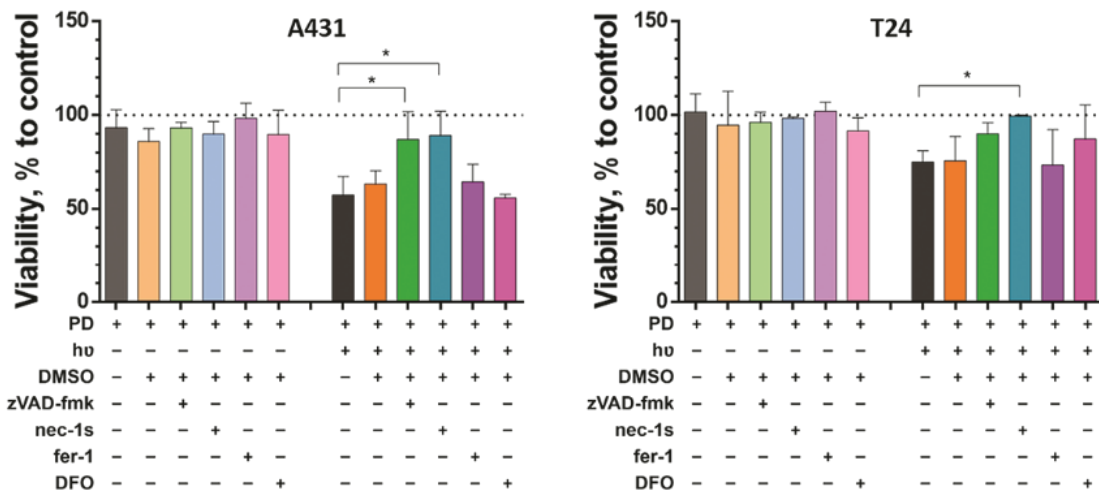


Fig. 4. Effect of different cell death inhibitors on A431 and T24 cells viability upon exposure to PD at a concentration of IC_{50} and irradiation (hv) at a dose of 20 J/cm^2 . The following inhibitors were used: $25 \mu\text{M}$ zVAD-fmk, $20 \mu\text{M}$ necrostatin-1s (nec-1s), $1 \mu\text{M}$ ferrostatin-1 (fer-1) and $10 \mu\text{M}$ deferoxamine (DFO). Cell viability of the untreated control (no PD or inhibitor) was set as 100% (dotted line). Error bars are represented by standard deviation ($n \geq 3$). *- Statistically significant difference between the indicated treatment options (t-criteria with Bonferroni correction, $p < 0.05$)

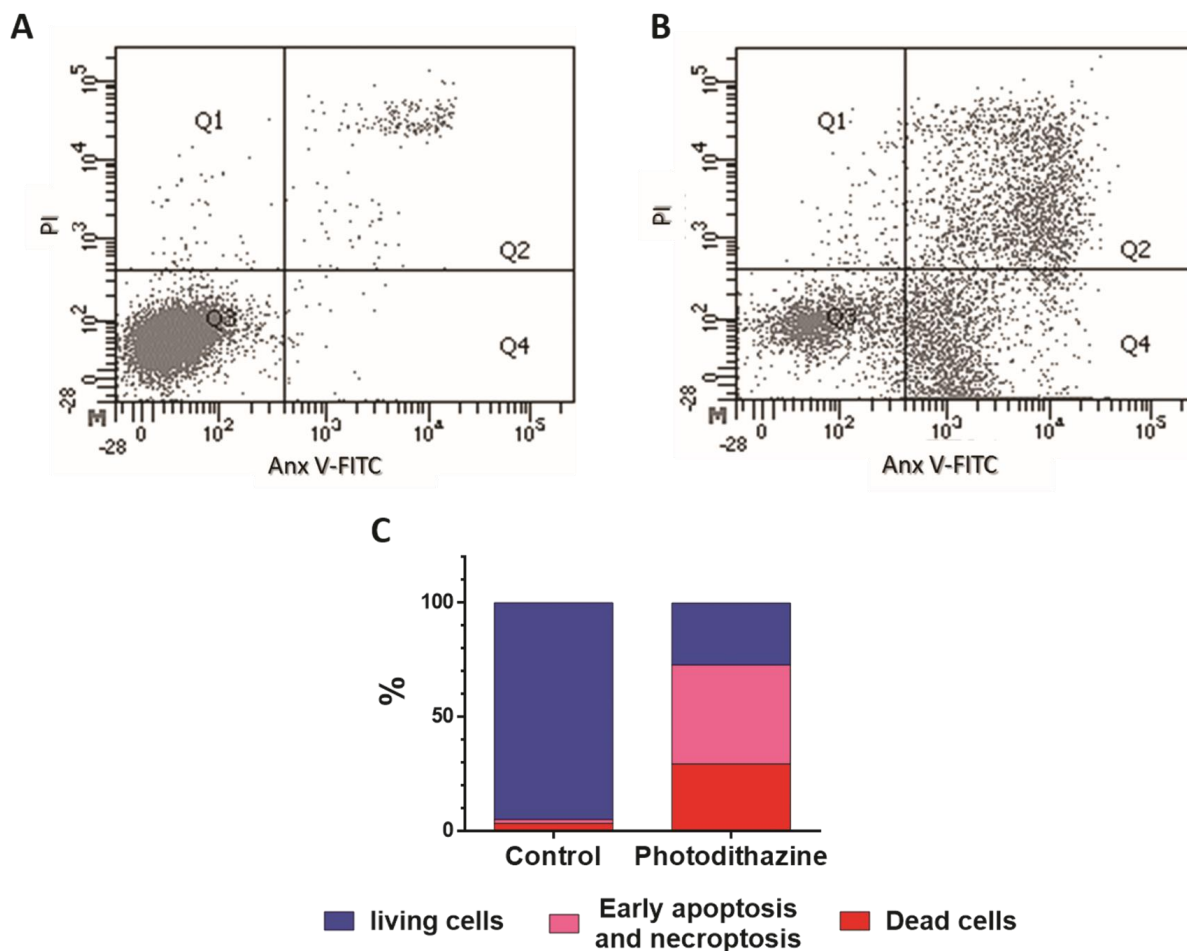


Fig. 5. Flow cytometry analysis the phosphatidylserine exposure on the external leaflet of the plasma membrane of A431 cells treated with PD at concentration of IC_{50} upon irradiation at a dose of $20 J/cm^2$. A431 cells were stained with PI and AnxV-FITC. (A) Untreated control (no PD); (B) A431 cells treated with PD; (C) The percentage distribution of A431 cells in the population of living cells (Anx^- , PI^-), early apoptotic and necroptotic cells (Anx^+ , PI^-) and dead cells (PI^+)

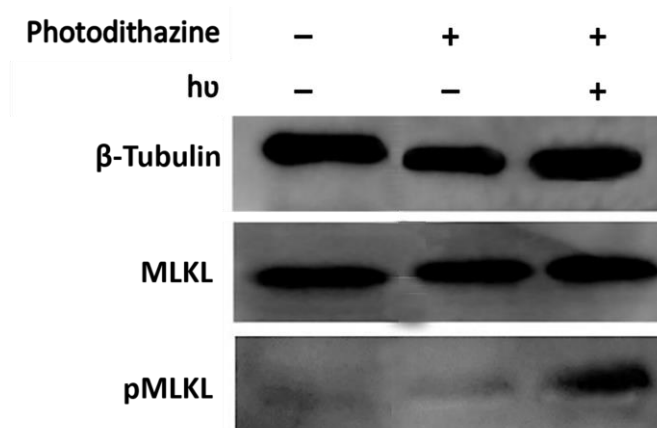


Fig. 6. Detection of the phosphorylated form of MLKL (pMLKL) in A431 cells treated with PD at concentration of IC_{50} upon irradiation (hu) at a dose of $20 J/cm^2$; β -tubulin was used as loading control. Western blot analysis was performed 13 h after irradiation

properties of PD determine its localization in different compartments, such as ER and Golgi apparatus. Therefore, the photodynamic effect of PD can cause ROS-mediated ER-stress and the Unfolded Protein Response (UPR) (Donohoe et al., 2019). The UPR induces the activation of the ER signaling proteins PERK, IRE1 α and ATF6, which results in apoptosis induction (Tabas & Ron, 2011). It has also been shown that disruption of microtubules or phosphorylation or cleavage of structural Golgi proteins, such as the structural protein of the Golgi apparatus GRASP65 and golgins, induce apoptosis (Machamer, 2015; He et al., 2020). To date, there are a number of studies showing the possibility of necroptosis induction in response to ER stress with the participation of RIPK1 kinase, but the detailed mechanisms of

this molecular pathway are not revealed yet (Kishino et al., 2019; Mohammed Thangameeran et al., 2020).

Thus, based on dying cell morphology, exposure of phosphatidylserine on to the cell surface, presence of pMLKL and protective action of pan-caspase inhibitor and inhibitor of RIPK1, we hypothesize that Photodithazine forces cells to enter mixed-type cell death with features of apoptosis and necroptosis.

Acknowledgments

This research was supported by the Russian Foundation for Basic Research (Grant № 18-44-520010) and the Ministry of Education and Science of the Russian Federation (Agreement № 0729-2020-0061).

References

- ABRAHAMSE H. & HAMBLIN M.R. (2016): New photosensitizers for photodynamic therapy. *Biochem. J.*, 473, 347–364.
- BACELLAR I.O., TSUBONE T.M., PAVANI C. & BAPTISTA M.S. (2015): Photodynamic efficiency: From molecular photochemistry to cell death. *Int. J. Mol. Sci.*, 16(9), 20523–20559.
- BRILKINA A. A., PESKOVA N. N., DUDENKOVA V. V., GOROKHOVA A. A., SOKOLOVA E. A. & BALALAEVA I. V. (2018): Monitoring of hydrogen peroxide production under photodynamic treatment using protein sensor HyPer. *Journal of Photochemistry and Photobiology B: Biology*. 178, 296–301.
- CASTANO A.P., DEMIDOVA T.N. & HAMBLIN M.R. (2004): Mechanisms in photodynamic therapy: Part one-photosensitizers, photochemistry and cellular localization. *Photodiagn. Photodyn. Ther.*, 1(4), 279–293.
- DHURIYA Y.K. & SHARMA D. (2018): Necroptosis: a regulated inflammatory mode of cell death. *J Neuroinflammation*. 15, 199.
- DOLMANS D.E., FUKUMURA D. & JAIN R.K. (2003): Photodynamic therapy for cancer. *Nat. Rev. Cancer*. 3(5), 380–387.
- DONOHOE C., SENGE M.O., ARNAUT L.G., GOMES-DA-SILVA L.C. (2019): Cell death in photodynamic therapy: From oxidative stress to anti-tumor immunity. *Biochim Biophys Acta Rev Cancer*. 1872(2), 188308.
- DOS SANTOS A.F., DE ALMEIDA D.R.Q., TERRA L.F., BAPTISTA M.S. & LABRIOLA L. (2019): Photodynamic therapy in cancer treatment - an update review. *J. Cancer Metastasis Treat*. 5, 25.
- DOS SANTOS A.F., INAGUE A., ARINI G.S., TERRA L.F., WAILEMANN R.A.M., PIMENTEL A.C., YOSHINAGA M.Y., SILVA R.R., SEVERINO D., DE ALMEIDA D.R.Q., GOMES V.M., BRUNICARDOSO A., TERRA W.R., MIYAMOTO S., BAPTISTA M.S. & LABRIOLA L. (2020): Distinct photo-oxidation-induced cell death pathways lead to selective killing of human breast cancer cells. *Cell Death Dis*. 11(12), 1070.
- GARG A.D., DUDEK A.M., FERREIRA G.B., VERFAILLIE T., VANDENABEELE P., KRYSKO D.V., MATHIEU C. & AGOSTINIS P. (2013): ROS-induced autophagy in cancer cells assists in evasion from determinants of immunogenic cell death. *Autophagy*. 9, 1292–1307.
- GREER A. (2006): Christopher Foote's discovery of the role of singlet oxygen [1O₂ (1 Δ g)] in photosensitized oxidation reactions. *Accounts of Chemical Research*, 39(11), 797–804.
- HAMBLIN M.R. (2020): Photodynamic Therapy for Cancer: What's Past is Prologue. *Photochem Photobiol*. 96(3), 506-516.

- HE Q., LIU H., DENG S., CHEN X., LI D., JIANG X., ZENG W. & LU W. (2020): The Golgi Apparatus May Be a Potential Therapeutic Target for Apoptosis-Related Neurological Diseases. *Front Cell Dev Biol.* 8, 830.
- JUARRANZ A., JAEN P., SANZ-RODRIGUEZ F., CUEVAS J. & GONZALEZ S. (2008): Photodynamic therapy of cancer. Basic principles and applications. *Clin. Transl. Oncol.* 10, 148–154.
- KISHINO A., HAYASHI K., MAEDA M., JIKE T., HIDAI C., NOMURA Y. & OSHIMA T. (2019): Caspase-8 Regulates Endoplasmic Reticulum Stress-Induced Necroptosis Independent of the Apoptosis Pathway in Auditory Cells. *Int J Mol Sci.* 20(23), 5896.
- KRAMMER B. (2001): Vascular effects of photodynamic therapy. *Anticancer Res.* 6B, 4271–4277.
- MACHAMER C.E. (2015): The Golgi complex in stress and death. *Front Neurosci.* 9, 421.
- MOHAMMED THANGAMEERAN S.I., TSAI S.T., HUNG H.Y., HU W.F., PANG C.Y., CHEN S.Y. & LIEW H.K. (2020): A Role for Endoplasmic Reticulum Stress in Intracerebral Hemorrhage. *Cells.* 9(3), 750.
- MROZ P., SZOKALSKA A., WU M.X. & HAMBLIN M.R. (2010): Photodynamic therapy of tumors can lead to development of systemic antigen-specific immune response. *PLoS ONE.* 5(12), e15194.
- ROBERTSON C.A., EVANS D.H. & ABRAHAMSE H. (2009): Photodynamic therapy (PDT): A short review on cellular mechanisms and cancer research applications for PDT. *Journal of Photochemistry and Photobiology B: Biology*, 96, 1–8.
- SAMSON A.L., ZHANG Y., GEOGHEGAN N.D., GAVIN X.J., DAVIES K.A., MLODZIANOSKI M.J., WHITEHEAD L.W., FRANK D., GARNISH S.E., FITZGIBBON C., HEMPEL A., YOUNG S. N., JACOBSEN A.V., CAWTHORNE W., PETRIE E.J., FAUX M.C., SHIELD-ARTIN K., LALAOUI N., HILDEBRAND J.M., SILKE J. & MURPHY J.M. (2020): MLKL trafficking and accumulation at the plasma membrane control the kinetics and threshold for necroptosis. *Nature communications.* 11(1), 3151.
- SEGAWA K. & NAGATA S. (2015): An Apoptotic 'Eat Me' Signal: Phosphatidylserine Exposure. *Trends Cell Biol.* 25(11), 639-650.
- SHAMS M., OWCZARZAK B., MANDERSCHIED-KERN P., BELLNIER D.A. & GOLLNICK S.O. (2015): Development of photodynamic therapy regimens that control primary tumor growth and inhibit secondary disease. *Cancer Immunol. Immunother.* 64, 287–297.
- SHILYAGINA N.Y., PLEKHANOV V.I., SHKUNOV I.V., SHILYAGIN P.A., DUBASOVA L.V., BRILKINA A.A., SOKOLOVA E.A., TURCHIN I.V. & BALALAEVA I.V. (2014): LED light source for in vitro study of photosensitizing agents for photodynamic therapy. *Sovremennye Tehnologii v Med.* 6(2), 15–22.
- SHLOMOVITZ I., SPEIR M. & GERLIC M. (2019): Flipping the dogma – phosphatidylserine in non-apoptotic cell death. *Cell Commun Signal.* 17, 139.
- OLIVEIRA C.S., TURCHIELLO R., KOWALTOWSKI A.J., INDIG G.L. & BAPTISTA M.S. (2011): Major determinants of photoinduced cell death: Subcellular localization versus photosensitization efficiency. *Free Radic Biol Med.* 51(4), 824-833.
- TABAS I. & RON D. (2011): Integrating the mechanisms of apoptosis induced by endoplasmic reticulum stress. *Nat Cell Biol.* 13(3),184-190.
- TURUBANOVA V.D., BALALAEVA I.V., MISHCHENKO T.A., CATANZARO E., ALZEIBAK R., PESKOVA N.N., EFIMOVA I., BACHERT C., MITROSHINA E.V., KRYSKO O., VEDUNOVA M.V. & KRYSKO D.V. (2019): Immunogenic cell death induced by a new photodynamic therapy based on photosens and photodithazine. *J Immunother Cancer.* 7(1), 350.
- VAN STRATEN D., MASHAYEKHI V., DE BRUIJN H., OLIVEIRA S. & ROBINSON D. (2017): Oncologic Photodynamic Therapy: Basic Principles, Current Clinical Status and Future Directions. *Cancers.* 9(2), 19.
- WANG W., MORIYAMA L.T. & BAGNATO V.S. (2012): Photodynamic therapy induced vascular damage: an overview of experimental PDT. *Laser Phys. Lett.* 10, 023001.
- ZARGARIAN S., SHLOMOVITZ I., ERLICH Z., HOURIZADEH A., OFIR-BIRIN Y., CROKER B.A., REGEV-RUDZKI N., EDRY-BOTZER L. & GERLIC M. (2017): Phosphatidylserine externalization, "necroptotic bodies" release, and phagocytosis during necroptosis. *PLoS Biol.* 15(6), e2002711.
- ZHOU F., XING D. & CHEN W.R. (2009): Regulation of HSP70 on activating macrophages using PDT-induced apoptotic cells. *Int J Cancer.* 125(6), 1380–1389.